Liquidus Temperatures in the Ti-Al System

C.D. ANDERSON, W.H. HOFMEISTER, and R.J. BAYUZICK

Liquidus temperatures were determined for the titanium-aluminum system at compositions ranging from 41 to 62 at. pct Al. The measurements were obtained by inducing solidification of slightly undercooled melts under containerless processing conditions using electromagnetic levitation. Absolute temperatures were determined by optical pyrometry in combination with independent measurements of spectral emissivities by laser polarimetry. The present liquidus temperatures are in agreement with two sets of literature values and are consistent with a set of solid-state literature data. These values exceed those selected in one recent proposed phase diagram revision by about 30 K and are as much as 40 to 60 K higher than those in another proposed revision.

I. INTRODUCTION

TWO recently proposed titanium-aluminum binary phase diagram revisions exhibit important uncertainties that result from inaccurate liquidus temperature measurements.[1,2] For example, liquidus temperature data reported by different investigators span a range of 50 K in the near-equiatomic region of the diagram.[3,4,5] The characteristics of the Ti-Al system which have led to these uncertainties include reactions with containers and gaseous impurities, compositional shifts due to loss of the more volatile aluminum component, rapid solid-state phase transformations, and ambiguities in the room-temperature microstructures. As a result, the equilibrium phase diagram is still not completely understood even though many investigations of this system have been reported.[1-11]

The present research used containerless experimental techniques to determine accurate liquidus temperatures at near-equiatomic compositions in the titanium-aluminum system. These liquidus measurements were made possible by separate polarimetric measurements of liquid optical properties,[12] which allowed accurate correction of apparent temperatures measured with optical pyrometry. The results agree with previous results reported by Ogden *et al.*[3] and Kornilov *et al.*[5] but are in poor agreement with the liquidus data of Bumps *et al.*[4] and the liquidus curves used in two recent versions of the Ti-Al phase diagrams.[1,2]

II. EXPERIMENTAL

Specimens prepared from arc-cast ingots were levitated and melted inductively under an inert helium atmosphere. The apparent temperatures of the levitated liquid specimens were measured with an optical pyrometer. True temperatures were calculated from the apparent values and independently measured liquid emissivities. Liquidus temperatures were determined by inducing solidification in slightly undercooled (5 to 40 K) liquids.

C.D. ANDERSON, formerly Ph.D. Candidate, Department of Materials Science and Engineering, Vanderbilt University, is Research Scientist, Intersonics, Incorporated, Northbrook, IL 60062-1818. W.H. HOFMEISTER, Research Associate Professor, and R.J. BAYUZICK, Professor, are with the Department of Materials Science and Engineering, Vanderbilt University, Nashville, TN 37235.

Manuscript submitted March 27, 1992.

A. *Electromagnetic Levitation Processing*

The experiments were conducted in an apparatus described by Bertero *et al.*[13] The system was first evacuated to less than 5×10^{-5} torr (7×10^{-3} Pa) and filled to about one-half an atmosphere (5×10^{4} Pa) with cold-trapped, ultrahigh-purity (UHP) helium gas. Then a specimen was levitated, melted, heated above the melting point to clean the sample surface, and cooled with flowing UHP helium under a constant ambient pressure. The gas flow rate was adjusted to stabilize the apparent temperature, and nucleation was attempted by touching the sample with a pyrex whisker. If the sample was above the liquidus temperature, nucleation of the solid was thermodynamically impossible and did not occur, thereby providing an upper bound to the liquidus temperature. In such cases, the apparent temperature was reduced and the process repeated until nucleation occurred at some minimal undercooling, as indicated by the resulting small recalescence peak. The apparent liquidus temperature was then determined from the recalescence peak temperature and correlated with thermal arrest data obtained during melting.

B. *Noncontact Temperature Measurement*

The liquidus determinations in this work rely on noncontact temperature measurement techniques. A detailed description of the pyrometry calibration and measurement procedures is provided in the Appendix.

C. *Materials*

Samples for electromagnetic processing were cut from arc-cast ingots made from 99.99 pct pure Ti rods and 99.999 pct pure Al pellets (Aldrich Chemical Company, Milwaukee, WI). The arc-melting was conducted in UHP argon. Residual oxygen and nitrogen in the argon atmosphere were gettered prior to casting the ingots by melting pure specimens of titanim or zirconium metals. Each Ti-Al ingot was melted, rotated, and remelted at least four times.

Bulk compositions for all specimens were measured after electromagnetic processing by scanning electron microscopy/energy dispersive spectroscopy on a Hitachi X-650 Microanalyzer. Quantitative analyses were based on comparisons to alloy standard spectra using three

standard samples analyzed by wet chemistry at Allied-Signal Corporation, Morristown, NJ. The results for the standards were internally consistent and in agreement with EDS analysis using pure element standards.

Impurity analyses of specimens similar to those investigated were obtained prior to the present work. Analyses were made by Leco Corporation, St. Joseph, MI, and Allied-Signal Corporation for oxygen and hydrogen and by National Spectographic Laboratories, Cleveland, OH, for copper and tungsten. The latter two impurities might arise from the arc-melting process. Oxygen content was typically 600 ppm in as-received material and stayed approximately the same or decreased slightly during laboratory arc-melting. Oxygen content decreased by up to 100 ppm as a result of electromagnetic levitation melting. Hydrogen impurities were less than 15 ppm. The Cu and W levels were below detection limits, which were 100 ppm for Cu and 500 ppm for W. Analytical Associates, Detroit, MI, determined silicon and nitrogen impurity levels after electromagnetic processing. One sample was analyzed for silicon contamination, which might result from the use of pyrex whiskers to induce nucleation, and was found to contain 400 ppm. Nitrogen levels ranged from 20 to 200 ppm for several samples tested.

III. RESULTS

A. *Liquidus Temperatures*

Figure 1 contains typical uncorrected temperature *vs* time data for a deeply undercooled sample. Two apparent thermal arrests similar to those evident in the melting data were often seen in these experiments and are explained as follows. When the temperature began to arrest at about 86 seconds, the pyrometer spot was on a solid region of the sample. At about 91 seconds, the sample turned over so that liquid replaced solid in the field of view of the pyrometer. The liquid emissivity was somewhat higher (about 0.03 higher) than that of the solid, causing the apparent temperature to rise abruptly by about 12 K with no corresponding change in true temperature. After melting was complete at about 95 seconds, the sample overheated to about 1900 K at 105 seconds. At this time, cooling was begun by flowing helium across the sample surface. The sample cooled until spontaneous nucleation occurred at a nucleation temperature, T_N, of about 1470 K at 116 seconds. The resulting recalescence peak temperature, T_R, was about 1700 K. The apparent temperature inflection at about 112 seconds resulted from an increased gas flow rate.

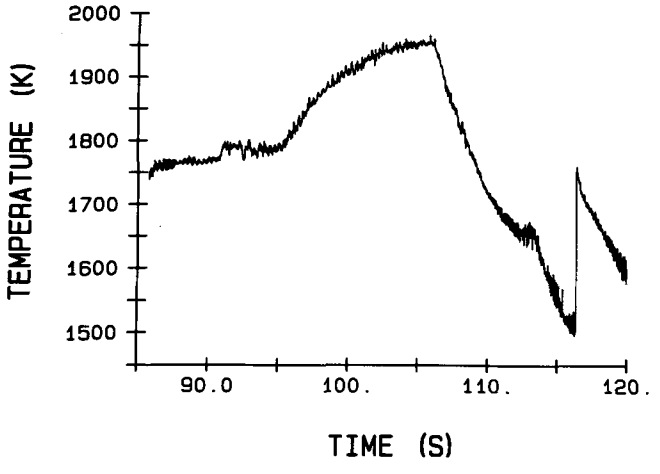

Fig. 1—Typical overall melting and recalescence cycle.

Recalescence peak temperatures on slightly bulk undercooled samples were used to determine liquidus temperatures. A representative temperature-time curve for these experiments is shown in Figure 2. A small temperature rise resulting from induced nucleation in the slightly undercooled (about 30 K) liquid can be seen at about 35.6 seconds. When a sample was undercooled by even a few degrees, recalescence was immediate and the stinger appeared macroscopically uneffected by contact with the sample. The stinger was sometimes wetted by the sample when it was touched above its liquidus temperature. On such occasions, the sample was assumed to be contaminated and was replaced.

Alloy compositions and liquidus temperature values are presented in Table I. The table includes values of the apparent temperatures measured with the optical pyrometer, the normal spectral emissivities, and the calculated

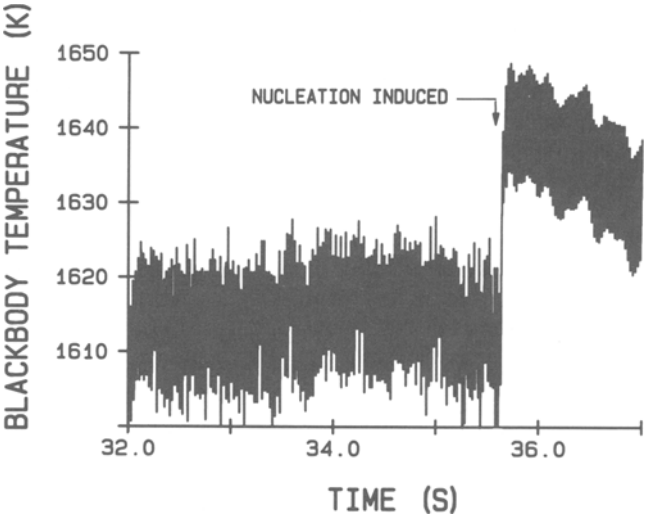

Fig. 2—Typical temperature *vs* time data showing recalescence resulting from induced nucleation of a slightly undercooled Ti-49.6 at. pct Al alloy.

Table I. Liquidus Temperatures for Titanium-Aluminum Alloys

At. Pct Al (±1.0)	T_a, K	Emissivity (±0.015)	T, K
41.6	1717 ± 6	0.320	1890 ± 10
44.5	1696 ± 6	0.324	1862 ± 10
49.4	1647 ± 8	0.332	1799 ± 11
51.3	1635 ± 8	0.333	1785 ± 11
54.3	1625 ± 8	0.324	1777 ± 11
56.5	1615 ± 8	0.318	1768 ± 11
58.9	1601 ± 8	0.311	1754 ± 11
61.4	1594 ± 10	0.301	1751 ± 14

true temperatures. The liquidus temperatures shown are equal to the recalescence peak temperatures that resulted from minimally undercooled samples. The use of these values was supported by melting data. The liquidus temperatures shown represent the assessed results of several measurements.

Figure 3 plots liquidus temperature *vs* composition for the near-equiatomic alloys. Three sets of literature data are also shown.[3,4,5] The present liquidus temperatures are in good agreement with the values of Ogden *et al.*[3] and Kornilov *et al.*[5] but exceed the values of Bumps *et al.*[4] by 35 to 55 K. Discontinuities in the liquidus curve drawn through the data are at compositions dictated by thermal and microstructural results obtained in a parallel study.[14] These compositions confirm the results of McCullough *et al.*[2] The first discontinuity occurs at 49.6 at. pct Al and results from the equilibrium primary solidification phase changing from β to α at the upper peritectic temperature, 1790 K. The second discontinuity is at about 56 at. pct Al and results from the primary solidification phase changing from α to γ at the lower peritectic temperature, 1755 K.

B. *Comparison with Solid-State Data from Literature*

Figure 4 contains the high-temperature near-equiatomic phase diagram that would result from the combination of the present data with the solid-state data of McCullough *et al.*[2] The two sets of data combine to form phase boundaries that obey the phase rules and are reasonable in form. The presence of the $\alpha + L$ phase field between the $\beta + L$ and $\gamma + L$ phase fields was determined in a parallel study[14] and is in agreement with several recent studies (*e.g.*, References 2, 15, and 16).

C. *Accuracy of Liquidus Measurements*

The near-equiatomic Ti-Al liquidus exhibits a relatively small dependence of temperature on composition, *i.e.*, 140 K in the 41.6 to 61.4 at. pct Al composition

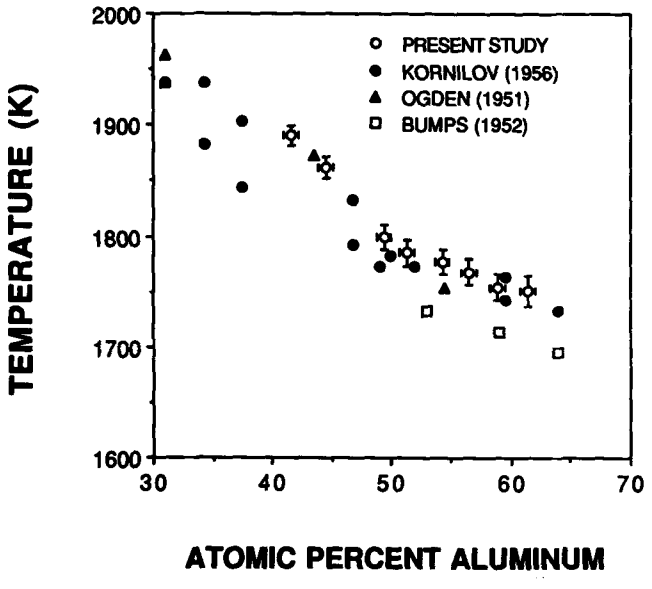

Fig. 3—Liquidus results for near-equiatomic Ti-Al alloys.

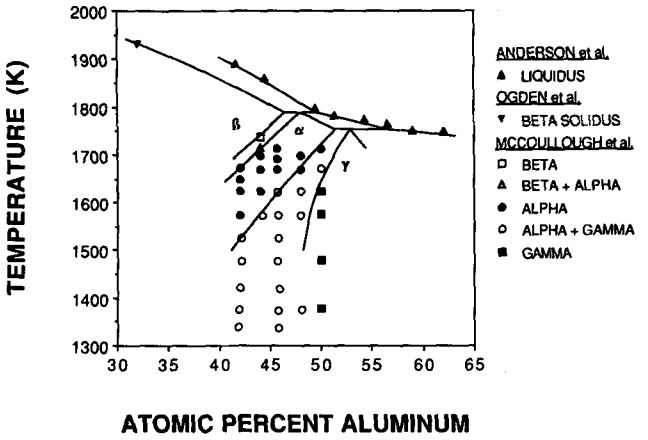

Fig. 4—Present liquidus temperatures plotted with solid-state data of McCullough *et al.*[2]

range investigated in this work. This means that the ±1 at. pct Al uncertainty composition has only a small influence on the liquidus temperature. Therefore, the accuracy with which the near-equiatomic liquidus has been determined depends almost entirely on the accuracy of the temperature measurements. The situation is quite different for compositions near pure aluminum, where the liquidus temperature can change by over 100 K for a change of 1 at. pct Al in liquidus composition.

The true recalescence peak temperatures were determined from the apparent peak temperatures using liquid spectral emissivities. Melting data indicate that this procedure would result in an underestimation of the recalescence temperatures by 10 to 15 K if the pyrometer field of view were filled with solid rather than liquid. In the present study, this error was reduced greatly by inducing nucleation at small bulk undercoolings at a point on the sample directly opposite the pyrometer field of view. This procedure ensured that even if solidification were to occur with a concave front (as indicated by the modeling of Levi on small aluminum spheres[17]), the field of view would encompass only a small fraction of solid immediately upon reaching the recalescence peak temperature.

The fact that only a small fraction of the sample was solid at the conclusion of recalescence also ensured that the change in liquid composition due to solute rejection during recalescence was negligible. For the near-equiatomic compositions, the liquid would be enriched by at most a few tenths of an at. pct Al for a sample bulk undercooled by 30 K. Thus, the liquidus temperature would be decreased by a maximum of about 2 K by compositional changes during recalescence in the experiments from which the liquidus was determined.

In a typical experimental run, the mass of a 300 mg sample decreased by about 0.6 mg. The exact amount depended on the degree of overheat and the time at temperature. All of the mass loss is attributed to vaporization of aluminum, because the vapor pressure of titanium relative to aluminum is negligible at the temperatures of interest. The typical mass loss corresponds to a lowering of the Al content by about 0.3 at. pct per run for an equiatomic alloy.

Spectral emissivities used to calculate true temperatures from the apparent temperatures measured with the pyrometer were calculated by linear interpolation between compositions for which the values were known to better than ±0.01 at a wavelength of 633 nm.[12] A total emissivity uncertainty of ±0.015 was estimated for the present work to account for additional errors resulting from (1) differences that may exist between 633 nm and the bandpass of the pyrometer (centered at 645 nm), (2) the fraction solid in the pyrometer field of view and its effect on apparent temperature, and (3) possible interpolation errors. For the temperature range of interest in these studies, an error of 0.015 in emissivity results in about a 6 K error in true temperature.

The reproducibility of the apparent liquidus temperature measurements was affected mainly by the magnitude of specimen oscillations which developed when nucleation was induced. For small undercoolings, the exact level of undercooling had little effect on the results; on a Ti-51 at. pct Al sample, the liquidus temperature was reproduced to ±2 K for undercoolings up to 50 K.

The uncertainties in the liquidus temperature were determined as the quadratic sums of individual values resulting from pyrometer calibration (±5 K), emissivity (±6 K), and reproducibility of liquidus apparent temperature measurements (±6 to 10 K).

IV. DISCUSSION

A. *Liquidus Temperature Measurement*

The present work has achieved liquidus temperature measurements by observing solidification and by conducting the experiments under containerless conditions. This approach solved two conceptual problems which exist in the techniques used in previous work to determine the Ti-Al liquidus curve by observing the melting of specimens in containers. The first problem is that dissolution of container-deprived impurities can significantly depress the melting point. For example, if liquid Ti contained 1 pct of an impurity which did not dissolve in the solid, the Vant Hoff relationship (*e.g.*, Reference 18) would show the melting point to be depressed by approximately 20 K. The second problem is that interdiffusion of Ti and Al in the solid is too slow to allow equilibrium solid compositions during the incongruent melting which occurs for near-equiatomic alloys.

The highest observed nucleation temperature for an alloy is the lower bound for the liquidus at the bulk composition. The lowest unsuccessful nucleation attempt in the overheated liquid is the upper bound. It was found by bracketing a small number of samples that the peak temperature resulting from recalescence in a slightly undercooled drop was a good approximation of the liquidus temperature. Therefore, the recalescence peak temperatures can be taken as accurate measures of the liquidus temperature for each sample bulk composition, independent of solid phase equilibration and container interaction effects.

B. *Cleaning of the Alloy Surfaces*

Krishnan *et al.* have demonstrated that containerless heating and melting of titanium and aluminum yield clean, bright surfaces on the resulting metals.[19] Under the reducing conditions that exist with the liquid metals present, volatile oxide vapors TiO and Al_2O are produced which remove the oxides from the metal surface.

Oxides were removed from alloy surfaces in the present work after heating to temperatures less than 2000 K even though temperatures of over 2000 K are required to clean oxide from pure Ti. This occurred because oxygen evaporates much more readily from the alloy as gaseous Al_2O molecules than from the pure metal as gaseous TiO molecules.

Aluminum and titanium nitrides are more difficult to remove from metal surfaces than oxides.[19] Nevertheless, the absence of nitrides from the liquid alloy surfaces in the present work was indicated by the bright metal luster of specimens recovered from the experiments and the large undercoolings (about 20 pct of melting) that were achieved in a parallel study[14] under conditions the same as in the present work. This indicates that solid impurity phases, which would tarnish the surface and serve as heterophase nucleants, were absent from the surface. Thus, nitrogen either decomposed from the surface, dissolved in the liquid, or was never present.

C. *The Assessed Ti-Al Liquidus Curve*

Murray[1] has assessed the Ti-Al phase diagram. The liquidus curve she proposed was based on data that existed prior to 1985. The present near-equiatomic liquidus curve is about 30 K above that shown by Murray.

The liquidus curve derived by Murray[1] and the data upon which it was based are shown in Figure 2 of her article. In the near-equiatomic region, the curve was drawn at temperatures between those of Bumps *et al.*[4] and Kornilov *et al.*[5] and is consistent with liquidus data near the $TiAl_3$ composition reported by Manchot and Leber.[20]

In fact, Bumps *et al.*[4] made only three liquidus temperature measurements and stated that the thermal analysis did not give a definite indication of the melting range. Most of the data points of Bumps *et al.* and a few of the data points of Kornilov *et al.*[5] were actually solidus values. Inclusion of these points biased the assessed liquidus toward lower temperatures. A more accurate assessment would accept Kornilov *et al.*'s data which agree with the present results and with those of Ogden *et al.*[3] in the near-equiatomic regime.

In addition to the near-equiatomic values, Kornilov *et al.*[5] also reported liquidus temperatures for compositions near $TiAl_3$. These values exceed those of Manchot and Leber[20] by 50 K. The temperatures reported by Manchot and Leber are also too small at high aluminum concentrations, where their value at 98.3 at. pct Al is 160 K less than the well-established liquidus curve in this compositional regime.[21–24] Melting point depression by contaminants is the likely cause of these discrepancies. The specimens investigated by Manchot and Leber (in 1926) were prepared by *in situ* synthesis of Ti-Al alloys from K_2TiF_6-Al mixtures surrounded by Al_2O_3 powder in a MgO crucible. Nitride contamination was suspected, because TiN features were observed in the microstructures. The data of Manchot and Leber negatively influence the way in which the Al-rich half of the phase diagram is interpreted and should be rejected.

McCullough *et al.*[2] proposed a near-equiatomic Ti-Al phase diagram based on high-temperature X-ray diffraction data and microstructural examinations of dendrite secondary arm orientations. The former experiments were used to determine the high-temperature solid phase boundaries, while the latter were used to determine peritectic liquidus compositions.[2] The solid/liquid phase fields established by McCullough are in doubt due to uncertain liquidus temperature data. However, the solid-state data, when combined with the present liquidus curve, result in a near-equiatomic phase diagram that appears reasonable (Figure 4).

Since Murray's[1] assessment, additional Ti-Al liquidus values have been reported in the literature. Schuster and Ipser obtained liquidus temperatures for the range from Ti-58 to Ti-76 at. pct Al using differential thermal analysis.[25] The derived liquidus curve is about 20 K below that from the present study at Ti-60 at. pct Al, with the upper bound from Schuster and Ipser approximately equal to the lower bound from the present work. The curve of Schuster and Ipser is in approximate agreement with Kornilov *et al.*[5] at $TiAl_3$ and therefore supports the rejection of the Manchot and Leber[20] data. The results of Mishurda and Perepezko from 40 to 75 at. pct Al,[16,26] also by DTA, are about 20 to 35 K below the liquidus values derived in the present work but are in approximate agreement with Kornilov *et al.* at $TiAl_3$. Huang and Siemers[15] analyzed microstructures after heat-treatment experiments in sealed capsules to derive liquidus temperatures for the range from 50 to 55 at. pct Al. This technique, which is highly susceptible to contamination at high temperatures, yielded liquidus temperatures that are about 40 to 50 K below the present values.

The values reported herein are slightly higher than some of the previous results. This is not surprising given the high reactivity of Ti-Al alloys and the fact that all previous experiments were conducted in containers. Contamination results in the depression of the true melting point of these alloys and an underestimation of the liquidus curve.

ACKNOWLEDGMENTS

This work was sponsored by the NASA Microgravity Science and Applications Division under Contract Nos. NAG8-765 and NAS8-37472 and by the NASA Office of Commercial Programs under Contract No. NAGW-810. The authors wish to thank Shankar Krishnan, Richard Weber, and Paul Nordine of Intersonics, Incorporated for the use of Intersonics' equipment and their expertise in conducting the emissivity experiments; they also thank David Skinner of Allied-Signal Corporation for help with chemical analysis. Dr. Nordine deserves additional thanks for analyzing the thermodynamics of impurities.

APPENDIX

Noncontact apparent temperature measurement

In general, the radiometric measurement equation is given as[27]

$$S = \int_{\lambda}\int_{\omega}\int_{A_t} R(\lambda)\tau(\lambda)L_{\lambda}(\lambda,T)\partial A_t \cos\theta\partial\omega_t\partial\lambda \quad [1]$$

where S is the signal intensity, λ is the wavelength, ω is the solid angle subtended by the detector (defined by the field limiting aperture), A_t is the target area, θ is the angle between the target surface normal and the optical axis, $R(\lambda)$ is the responsivity of the detector as a function of wavelength, $\tau(\lambda)$ is the transmissivity of the optical path, T is the thermodynamic or "true" temperature, and $L_{\lambda}(\lambda,T)$ is the spectral radiance of the target. For a narrow bandpass pyrometer with a well-defined optical path, Eq. [1] can be reduced to

$$S = \int_{\lambda} K(\lambda)L_{\lambda}(\lambda,T)\partial\lambda \quad [2]$$

where $K(\lambda)$ is the instrument constant which includes the responsivity of the detector and the transmissivity and geometry of the optical path.

The blackbody spectral radiance, $L_{\lambda b}$, for the spectral bandpass of the pyrometer in the temperature range of interest can be represented by the Wein approximation to Planck's Law.

$$L_{\lambda b}(T) = \frac{C_1}{\lambda^5}\exp\left(-\frac{C_2}{\lambda T_a}\right) \quad [3]$$

where C_1 and C_2 are Planck's radiation constants and T_a is the "apparent" or "brightness" temperature (Note that for a blackbody emitter, T_a is equal to the true temperature. For a real surface, T_a is less than T). In practice, when the pyrometer bandpass is sufficiently narrow, it is useful to define an effective wavelength such that the integrals of Eqs. [1] and [2] over the bandpass of the instrument are equal to their respective integrands.[28] The resulting blackbody pyrometer equation is

$$S = K\frac{C_1}{\lambda_{eff}^5}\exp\left(\frac{-C_2}{\lambda_{eff}T_a}\right) \quad [4]$$

For a real surface, the spectral radiance at any true temperature is equal to the product of the blackbody spectral radiance and the normal spectral emissivity, ε_{λ}. Thus, for a real surface, Eq. [4] becomes

$$S = \varepsilon_{\lambda}K\frac{C_1}{\lambda_{eff}^5}\exp\left(-\frac{C_2}{\lambda_{eff}T}\right) \quad [5]$$

In general, ε_{λ} is a function of wavelength, temperature, and composition.

The true temperature of a real surface can be calculated from the measured apparent temperature. The following relationship is found by equating Eqs. [4] and [5]:

$$\frac{1}{T} = \frac{1}{T_a} + \frac{\lambda_{eff}}{C_2}\ln\varepsilon_{\lambda} \quad [6]$$

Apparent temperatures of levitated samples were measured with a dual-purpose, single color pyrometer.[29] The Gaussian filter used in this pyrometer had a 70 nm bandpass centered at 645 nm. The effective wavelength and instrument constant were determined using a tungsten strip

lamp (#P114), obtained from the National Institute of Standards and Technology, Gaithersburg, MD. This lamp was calibrated at 655 nm to IPTS-68 and has a stated 3 σ accuracy of ± 3 K. Since the lamp was calibrated at 655 nm and the pyrometer bandpass was centered at 645 nm, a slight correction was necessary. From Eq. [6] and the tungsten $\varepsilon(\lambda)$ data of Larrabee,[30] this correction was found to be +0.77 K at 1173 K and +2.0 K at 1873 K. The lamp was observed by the pyrometer at several temperatures in the range of interest through an optical path identical to that used in the experiments. The fact that the output of the silicon detector is linear with incident power allowed λ_{eff} to be determined graphically from a plot of the natural log of detector voltage *vs* $1/T$. The slope of this line is $-\lambda_{eff}/C_2$. The instrument constant, K, was then calculated by inserting λ_{eff} into Eq. [4] with calibration voltages and temperatures. For the pyrometer used in the present study, the effective wavelength and instrument constant were found to be 672.4 nm and 5.953×10^{-11} m^3 s C^{-1}, respectively. Using Eq. [4], the calibration temperatures at 645 nm could be reproduced to ± 0.5 K. This effective wavelength was confirmed by integration of Eq. [2] over the measured bandpass of the filter with the published responsivity curve of the detector.

Normal spectral emissivities determined with plane-polarized ellipsometry in a parallel study were used to determine true temperatures from the measured apparent temperatures. In this study, emissivity values at 632.8 nm were found for several binary Ti-Al liquid alloys at temperatures both above and below the liquidus.[12]

The pyrometer calibration was checked *in situ* by observing the melting and solidification of pure nickel several times during the course of the experiments. The apparent melting temperature of nickel was 1602 to 1603 K which translates to 1721 K using an emissivity of 0.40 at 633 nm[31] and 1731 K using an emissivity of 0.37 at 650 nm.[32] The published values for the melting point of nickel, which vary from 1726[33] to 1728,[34] fall well within this range.

REFERENCES

1. J.L. Murray: "Binary Titanium Alloy Phase Diagram Compilation," Final Technical Report to the Office of Naval Research, Project No. N00014-85-F-0069, 1985.
2. C. McCullough, J.J. Valencia, C.G. Levi, and R. Mehrabian: *Acta Metall.*, 1989, vol. 37, p. 1321.
3. H.R. Ogden, D.J. Maykuth, W.L. Finlay, and R.I. Jaffe: *Trans. AIME*, 1951, vol. 191, pp. 1150-55.
4. E.S. Bumps, H.D. Kessler, and M. Hansen: *Trans. AIME*, 1952, vol. 194, pp. 609-14.
5. I.I. Kornilov, E.N. Pylaeva, and M.A. Volkova: *Izv. Akad. Nauk SSSR, Otd. Khim. Nauk*, 1956, vol. 7, pp. 771-80 (in Russian).
6. F.A. Crossley: *Trans. TMS-AIME*, 1966, vol. 263, p. 1174.
7. M.J. Blackburn: *Trans. AIME*, 1967, vol. 239, pp. 1200-08.
8. E.W. Collings: *Metall. Trans. A*, 1979, vol. 10A, pp. 463-74.
9. T.K.G. Namboodhiri: *Mater. Sci. Eng.*, 1983, vol. 57, p. 21.
10. L.J. Swartzendruber, L.H. Bennett, L.K. Ives, and R.D. Shull: *Mater. Sci. Eng.*, 1981, vol. 51, pp. P1-P9.W.
11. R.D. Shull, A.J. McAlister, and R.C. Reno: *Phase Equilibria in the Titanium-Aluminum System*, 5th Int. Conf. on Titanium, Munich, Federal Republic of Germany, 1984, vol. 3, p. 1459.
12. S. Krishnan, C.D. Anderson, J.K.R. Weber, P.C. Nordine, W.H. Hofmeister, and R.J. Bayuzick: *Metall. Trans. A*, 1993, vol. 24A, pp. 67-72.
13. G.A. Bertero, W.H. Hofmeister, M.B. Robinson, and R.J. Bayuzick: in *Materials Processing in Space*, N.B. Singh, V. Laxmanan, and E.W. Collings, eds., Materials Science Forum, Trans. Tech. Ltd., Aedermannsdorf, Switzerland, 1989, vol. 50, p. 173.
14. C.D. Anderson, W.H. Hofmeister, and R.J. Bayuzick: *Metall. Trans. A*, 1992, vol. 23A, pp. 2699-2714.
15. S.C. Huang and P.A. Siemers: *Metall. Trans. A*, 1989, vol. 20A, pp. 1899-1906.
16. J.C. Mishurda, J.C. Lin, Y.A. Chang, and J.H. Perepezko: in *High-Temperature Ordered Intermetallic Alloys III*, C.T. Liu, A.I. Taub, N.S. Stoloff, and C.C. Koch, eds., MRS Symp. Proc., Materials Research Society, Pittsburgh, PA, 1989, vol. 133, pp. 57-62.
17. C.G. Levi and R. Mehrabian: *Metall. Trans. A*, 1982, vol. 13A, pp. 221-34.
18. G.N. Lewis and M. Randall: *Thermodynamics*, 2nd ed., McGraw-Hill Book Company, New York, NY, 1961, p. 173.
19. S. Krishnan, J.K.R. Weber, P.C. Nordine, R.A. Schiffman, R.H. Hauge, and J.L. Margrave: *High Temp. Sci.*, 1991, vol. 30, pp. 137-53.
20. W. Manchot and A. Leber: *Z. Anorg. Chem.*, 1926, vol. 150, pp. 26-34 (in German).
21. W.L. Fink, K.R. Van Horn, and P.M. Budge: *Trans. AIME*, 1939, vol. 93, pp. 421-39.
22. M. Heckler: *Aluminum*, 1974, vol. 50 (6), pp. 405-07 (in German).
23. K. Shibata, T. Sato, and G. Ohira: *J. Cryst. Growth*, 1978, vol. 44, pp. 435-45.
24. A. Abdel-Hamid, C.H. Allibert, and F. Durand: *Z. Metallkd.*, 1984, vol. 76, pp. 455-58.
25. J.C. Schuster and H. Ipser: *Z. Metallkd.*, 1990, vol. 81, p. 389.
26. J.C. Mishurda and J.H. Perepezko: in *Microstructure/Property Relationships in Titanium Aluminides and Alloys*, Young-Won Kim and Rodney R. Boyer, eds., TMS, Warrendale, PA, 1991, pp. 3-30.
27. G.D. Nutter: "Applications of Radiation Pyrometry," ASTM STP 895, 1985.
28. H.J. Kostkowski and R.D. Lee: *Proc. 4th Symp. on Temperature, Its Measurement and Control in Science and Industry*, Columbus, OH, March 27–31, 1961, Reinhold Publishing Co., New York, NY, 1961, p. 1.
29. W.H. Hofmeister, R.J. Bayuzick, and M.B. Robinson: *Rev. Sci. Instrum.*, 1990, vol. 61, p. 2220.
30. R.D. Larrabee: *J. Opt. Soc. Am.*, 1959, vol. 49, p. 619.
31. S. Krishnan, G.P. Hansen, R.H. Hauge, and J.L. Margrave: *High Temp. Sci.*, 1990, vol. 29, p. 17.
32. W.F. Roeser and H.T. Wenzel: *Temperature, Its Measurement and Control in Science and Industry*, Reinhold Publishing Co., New York, NY, 1941.
33. *CRC Handbook of Chemistry and Physics*, 66th ed., Robert C. Weast, ed., CRC Press Inc., Boca Raton, FL, pp. 1985-86.
34. M.W. Chase, Jr., C.A. Davies, J.R. Downey, Jr., D.J. Frurip, R.A. McDonald, and A.N. Syugrud: *JANAF Thermochemical Tables*, 3rd ed., *J. Phys. Chem. Ref. Data*, 1985, vol. 14 (1).